Organic Photovoltaic Materials: Squarylium and Cyanine-TCNQ Dyes

Abstract: The photovoltaic properties of Schottky barrier sandwich cells consisting of sublimed and solution-cast thin films of selected squarylium (bis-anilino derivatives of cyclobuta-1,3-diene-2,4-dione) and cyanine-tetracyanoquinodimethanide (TCNQ) dyes have been measured. For hydroxy squarylium (OHSq), maximum power conversion efficiencies (η) were 0.2% for 850-nm light (1 mW/cm²); 0.05% for 633-nm light (94 mW/cm²); 0.06% for "white" light (21 mW/cm²); 0.15% for low intensity (0.14 mW/cm²) simulated AM0 light (sunlight under outer space conditions), and 0.02% for high intensity (140 mW/cm²) AM0 light. Efficiencies of selected OHSq cells were observed to increase fivefold when the cells were doped with bromine or 1-phenyl-3-p-N,N-diethylaminostyryl-5-p-N,N-diethylamino-phenyl-Δ²-pyrazoline (DEASP), e.g., 0.05 to 0.23% (Br); 0.004 to 0.021% (DEASP). The efficiency of a solution-cast cell of amorphous 2,2'-dicarbocyanine-TCNQ was 0.02% when 933-nm light (approximately 1 mW/cm²) was used. Amorphous solid solutions of 1,1'-diethyl-2,2'-dicarbocyanine- and oxa-2,2'-dicarbocyanine-TCNQ salts were also tested. The effects of various material and device properties on the performance of organic photovoltaic cells are discussed, and it is proposed that organic solar cells having efficiencies of one percent or more can be made by using existing technologies.

Introduction

Traditionally, new materials research for solar cell applications has been dominated by the inorganic semiconductor materials, silicon (Si) and gallium arsenide (GaAs), and influenced to a lesser extent by cadmium sulfide (CdS). These materials do indeed yield highly efficient photovoltaic devices whereby sunlight is converted directly into electricity. For example, doped single-crystal Si devices have attained conversion efficiencies as high as 18 percent [1], while more recent refinements of GaAs solar cells have produced the highest efficiencies reported for solar-electrical energy conversion: 22 percent [2]. In the case of Si and GaAs cells, the stringent purity requirements and the complicated device fabrication techniques cause such high device costs that the practical large-scale utilization of these photovoltaic cells is economically infeasible at this time. Sunlight concentration schemes may improve the economic outlook somewhat, but this is uncertain because concentrator costs are not fully known [3]. The CdS cells have generally been plagued by stability problems [4]. Most new research has, therefore, focused on various methods for reducing the cost of conventional Si and GaAs solar cells, principally through the use of amorphous and polycrystalline Si [5], polycrystalline GaAs [6], single-crystalline Si ribbon [7], and thin films of these materials.

A less popular approach to solar cell materials research has been the study of organic photoconductive compounds in the photovoltaic mode. These materials are potentially inexpensive and readily available, and device fabrication can be comparatively simple; for example, well-known spin-coating or dip-coating techniques might be possible. To date, the overwhelming barrier to the successful application of such organic devices has been their extremely poor conversion efficiencies [8-11], even under the best laboratory conditions. For example, exclusive of the systems discussed here [12, 13], the highest reported conversion efficiencies for undoped organic materials are 0.02% for chlorophyll [9], with low intensity monochromatic light (745 nm, 0.8 mW/cm²), and 0.001% with "white" light (unknown intensity) for magnesium phthalocyanine (MgPh) [10]. In general, these low power conversion efficiencies are attributable to low quantum efficiencies for charge generation, low carrier mobilities, high bulk resistivities, and trapping effects.

The technique of intentionally doping pure semiconductor materials with impurities to alter electronic properties (such as carrier lifetimes, bulk conductivities, mobilities, junction depths, etc.) is used extensively and is well understood in inorganic solar cell technology. With organic systems, however, the complex relation-

Copyright 1978 by International Business Machines Corporation. Copying is permitted without payment of royalty provided that (1) each reproduction is done without alteration and (2) the *Journal* reference and IBM copyright notice are included on the first page. The title and abstract may be used without further permission in computer-based and other information-service systems. Permission to *republish* other excerpts should be obtained from the Editor.

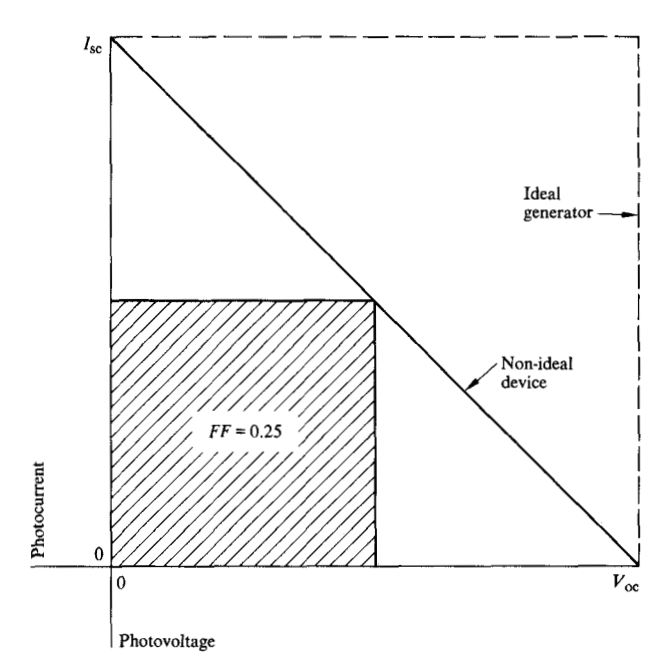


Figure 1 Schematic representation of fill factor FF.

ships among electronic properties and dopant types, concentrations, etc., are only just beginning to be studied. Dramatic changes in the photoconductive and photovoltaic properties of MgPh have been reported when the films were doped with oxygen [11]. These workers observed efficiency increases of one to three orders of magnitude for doped (as opposed to undoped) MgPh Schottky barrier cells. Unfortunately, their reported maximum power conversion efficiency of 0.1% has not yet been reproduced. Still, doping offers great potential for improving the efficiency of organic photovoltaic devices.

One basic argument exists: Even for solar cells with negligible material and fabrication costs, efficiencies of about ten percent must be attained if the cells are to be economically competitive with today's fossil-fuel-source electricity [14]. The same argument pertains to amorphous, polycrystalline, and thin-film Si and GaAs cells.

A systematic study of organic photovoltaic phenomena has led to formulation of a list of physical and chemical properties most likely required of potentially efficient organic photovoltaic materials. The concepts behind this list are discussed in the next section. The squarylium and cyanine-TCNQ dye systems were specifically chosen because they possessed or had the potential for possessing these key properties. For example, the amorphous or glassy state of these materials plays a key role in the improved absorption and transport properties observed. An investigation was also made of the various device parameters (e.g., film thickness, electrode couple, etc.) that

might affect cell performance because it was felt that the poor performance of previously studied organic systems might be due in large part to device (rather than material) limitations.

The results of these studies led this author to believe that, despite earlier reports of rather poor efficiencies, there are indeed organic photovoltaic systems capable of yielding power conversion efficiencies of one percent or more [13]. Thus, given a proper understanding of complex factors such as the "ohmicity" of the organic material-electrode interface, effects of dopants, and the delicate balances among conductivity, active barrier depth, and collection efficiencies, there are techniques that can be used to enhance the presently observed conversion efficiencies (0.1-0.2%) by approximately one order of magnitude. Even if competitive efficiencies (10%) are unattainable in the long run for organic systems, one can envision possible special-situation uses for organic photovoltaic cells.

Organic photovoltaic principles and material requirements

To predict the success or failure of a particular organic material used in the photovoltaic mode, it is necessary to understand the relationships between the various material and device properties and the overall cell performance. A brief summary of these relationships is presented here; however, good reviews exist that discuss photovoltaic principles in detail with regard to both inorganic and organic materials [9b, 15].

• Contact barriers and barrier height

The classical definition [8b] of a photovoltaic effect is the development of a voltage across an electrostatic potential barrier (here termed a *contact barrier*) by illumination. In a Schottky barrier photovoltaic cell, the contact barrier occurs between a metal and a semiconductor. Since most organic photovoltaic devices are of the Schottky barrier type, the discussion is limited to these cells.

Here, the power conversion efficiency η of a cell is used as the primary indication of the performance of that cell. The conversion efficiency is simply the ratio of the output power of the cell, $P_{\rm out}$, to the power *incident* on that cell, $P_{\rm in}$; η can be determined experimentally from the open-circuit voltage $V_{\rm oe}$, the short-circuit current $I_{\rm se}$ and active electrode area A (or the short-circuit current density $J_{\rm se}$), the fill factor FF, and the measurable input power as shown in Eq. (1):

$$\eta = \frac{P_{\text{out}}}{P_{\text{in}}} = \frac{V_{\text{oc}}I_{\text{sc}}FF}{AP_{\text{in}}} = \frac{V_{\text{oc}}J_{\text{sc}}FF}{\text{incident power density}}$$
 (1)

The fill factor is best described by referring to Fig. 1, which shows a photocurrent $(I_{\rm ph})$ -photovoltage $(V_{\rm ph})$ curve. For an ideal photovoltaic generator, the output $I_{\rm ph}$

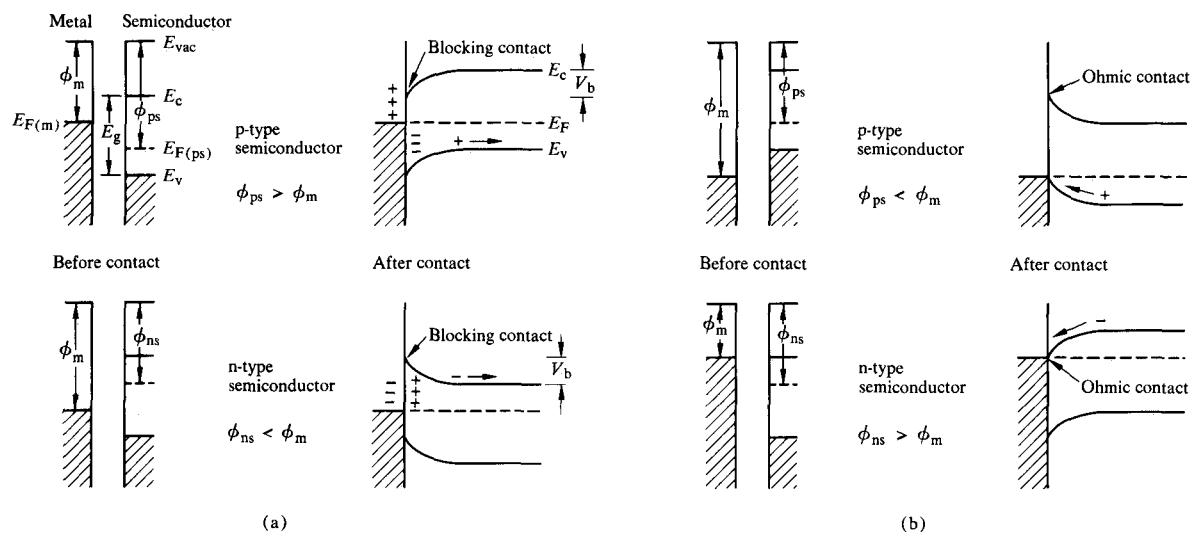


Figure 2 Schematic representation of energy band pictures for metal-semiconductor contacts. Blocking contacts (Schottky barriers) of potential V_b are in (a) whereas ohmic contacts are shown in (b). Notation is defined in the text.

is essentially independent of the output $V_{\rm ph}$; i.e., the curve is rectangular, and the maximum useful output power is simply the product of the maximum $V_{\rm ph} (=V_{\rm oc})$ and the maximum $I_{\rm ph} (=I_{\rm sc})$. This power can be represented by the total area under the curve. For non-ideal devices, however, the output $I_{\rm ph}$ decreases as the output $V_{\rm ph}$ increases; a plot of $V_{\rm ph}$ vs $I_{\rm ph}$ deviates from this rectangular shape. The intercept values of the voltage and current axes are $V_{\rm oc}$ and $I_{\rm sc}$, respectively. In these cases, the maximum useful output power is represented by the area of the largest rectangle that can be fit under the photo I-V curve. The fill factor is the ratio between this area and that represented by the ideal case ($I_{\rm sc} \times V_{\rm oc}$). In Fig. 2, the FF for the ideal generator is 1.00; for the non-ideal example shown (diagonal line), it is 0.25.

On the assumption that band theory is at least approximately applicable to organic semiconductors, where energy "bands" may not exist in a strict sense, a simplified analysis reveals that the maximum $V_{\rm oc}$ obtainable from a pure organic material in a Schottky barrier photovoltaic device is directly dependent upon the height of the energy (contact) barrier that is created between the organic material and the metal electrode. This contact barrier is, in turn, dependent upon the energy differences between the Fermi levels $(E_{\rm F})$ of the two materials, the positions of the conduction and valence band edges $(E_{\rm c}$ and $E_{\rm v}$, respectively) relative to the Fermi level of the organic material, and the bandgap $(E_{\rm g})$ of the latter.

In the example shown in Fig. 2(a), the Fermi level of the p-type organic semiconductor, $E_{\rm F(ps)}$, lies below that of the metal, $E_{\rm F(m)}$, relative to a common reference vacuum level ($E_{\rm vac}$). (See [9b] for a list of the conductivity classifications for common organic photoconductors.)

The difference between $E_{\rm vac}$ and $E_{\rm F}$ is also referred to as the work function ϕ . When these two materials are brought into contact, there is a flow of charge carriers across the boundary until one common $E_{\rm F}$ is attained at equilibrium. It is assumed here that an equilibrium (steady state) situation occurs within the time of the photovoltaic measurements. In addition, for the systems studied, the effects of space-charge-limited currents are minor; these effects become more pronounced at high intensities.

Depending upon the type of band-bending that occurs at this interface, one gets either a rectifying (blocking) contact of potential $V_{\rm b}$, an ohmic contact, or a neutral contact (not discussed); see Figs. 2(a-d). Rectifying contacts are formed when $\phi_{\rm ps} > \phi_{\rm m}$ or when $\phi_{\rm ns} < \phi_{\rm m}$. The electrical circuit for a photovoltaic device calls for one rectifying and one ohmic contact. If an ohmic contact is not present at the second electrode, the performance of the cell can be seriously reduced; this condition occurs frequently in organic systems. Ohmic contacts are formed when $\phi_{\rm ps} < \phi_{\rm m}$ or when $\phi_{\rm ns} > \phi_{\rm m}$.

A prime consideration for picking a potential photovoltaic material is, therefore, the relationship between the work functions of the organic and the two proposed electrode materials. The work functions of 40 or more organic photoconductors and dyes have been calculated from the data of various workers [9b, 10, 11, 16-21] and almost all fall between 3.3 and 5.2, with the vast majority occurring between 4.0 and 5.0. The work function of the two squarylium dyes studied, hydroxy squarylium, OHSq, and methyl squarylium, MeSq (bis-anilino derivatives of cyclo-buta-1,3-diene-2,4-dione), have been determined to be 4.15-4.20 and 4.5, respectively [21].

Theoretically, without a rectifying (Schottky) barrier, there can be no photovoltage, and the larger this barrier is, the larger the photovoltage can be; see, for example, [10, 16].

Surface states and impurities, however, alter the theoretical behavior of interfaces, as has just been described. In the band pictures for the isolated semiconductors shown in Fig. 2, the Fermi levels and the conduction and valence band edges were assumed to be uniform not only throughout the bulk of the material, but also at the surfaces. The presence of surface states, defects, or impurities can cause perturbations in the Fermi levels. A rise in the Fermi level (i.e., it now lies closer to the vacuum level and represents a decrease in the work function) can indicate an increase in electron density over that in the pure bulk material and a tendency to give up electrons more easily. For example, if surface states or impurities (dopants) exist that are either electron-rich (act as donors) or electron-poor (act as acceptors), an effective Fermi level, energetically different from the Fermi level of the pure bulk material, can be produced. A priori, the degree and direction of surface state or impurity band bending cannot always be easily predicted, and in fact, can also be different for similar material devices because of differences in sample history, etc. For these reasons it is possible to obtain experimental photovoltages that are inconsistent with theoretical values (see, for example, [10(b)], where a photovoltage was obtained for an Al/ chlorophyll/Al cell). When the surface of either the electrode material or the organic conductor is susceptible to oxidation, reduction, or other contamination, the cell must be carefully protected [22] if the photovoltaic properties of the pure organic material are to be studied. Such surface and impurity effects can also seriously affect the stability in time of organic photovoltaic systems. However, a device that performs reasonably well while not requiring special protection would be economically desirable.

As mentioned previously, it may be possible to utilize band-bending effects to enhance device performance of organic materials in the photovoltaic mode by means of intentional doping, partial oxidation of surfaces, etc. These concepts have been used in the study of organic metals such as (TTF)(TCNQ) and other conductive donor-acceptor salts [23]. In fact, it is likely that the best organic photovoltaic material will not be a pure compound, but will be doped in some manner.

• Depth of active barrier region

The active region of a contact barrier extends a finite distance into the organic material. This active region consists of a depletion region (barrier depth) and an effective diffusion depth, representing, respectively, the distance into the material that carrier generation occurs and an av-

erage distance over which these carriers can migrate before recombining or being trapped. The barrier depth W is dependent upon both the height of the contact potential barrier $V_{\rm b}$ and certain physical constants of the organic material. The diffusion depth L is dependent upon the carrier lifetime τ and the diffusion coefficient D for that carrier. Equations (2) and (3) give the proportionalities

$$W \propto (\epsilon V_{\rm b}/N_{\rm b})^{1/2} \tag{2}$$

where ϵ is the dielectric constant of the organic and $N_{\rm b}$ is the density of free carriers in the bulk of the organic; and

$$L \propto (D\tau)^{1/2}.\tag{3}$$

The presence of an electrostatic potential across the sample can affect the transport and collection of carriers within the organic material. If a sufficiently large potential drop exists, carrier diffusion is field-assisted, and the effective diffusion length is significantly increased; in extreme cases Eqs. (2) and (3) no longer hold. In addition, excitonic diffusion lengths may play a role; however, these are not discussed (see, e.g., [15]).

The active region in most organic photoconductors is extremely narrow, usually averaging 20-30 nm or less; this is mostly due to the large density of such trapping sites as impurities, defects, and grain boundaries, and to high bulk resistivities. Given a particular organic material, one can theoretically increase its performance in a Schottky barrier device by using a film thickness on the order of this active depth.

This optimal thickness (W+L) can be estimated by measuring the short-circuit current as a function of film thickness. If one assumes similar material and device histories, the maximal $I_{\rm sc}$ should occur near the optimal cell thickness. Another estimate of W+L can be made from the thickness at which backwall and frontwall response spectra (quantum efficiency vs wavelength) are the same and where they match the absorption spectrum of the organic material. Thus, thin films of organic materials would decrease the detrimental effects of high bulk resistivities; also, they would probably be the most efficient form of the materials in photovoltaic devices.

When comparing different organic materials for the purpose of finding potentially useful photovoltaic materials, one wants to maximize W + L by choosing materials with high dielectric constants, moderate bulk carrier densities (too high a density will cause a significant compression of W; too low a density will give an insulator), and good carrier mobilities and lifetimes.

• Absorption properties

An obvious extension of these principles concerns the energy absorption characteristics of various organic conductors. For solar cell applications, we are particularly

concerned with those wavelengths of light that are radiated by the sun (see Fig. 3; also [15(b)]).

If an organic conductor has an active depth of 30 nm, one must consider how many carriers can be generated in that region; this is determined by a distribution of wavelength-dependent absorption coefficients α for that material:

$$\alpha = -[\ln (R + T)]t^{-1}, \tag{4}$$

where t represents the film thickness, and T and R are the light transmission and reflectance, respectively. If one wants to absorb 95 percent of the incident light within a 30-nm depth, the average α for that distribution of wavelengths must be approximately 10^6 cm⁻¹. For most organic compounds, the average absorption coefficients are two to three orders of magnitude less than this, meaning that thicknesses of micrometers, rather than tens of nanometers, would be required to absorb 95 percent of the light. For certain classes of organic photoconductive dyes, α values of 10^5 to 10^6 cm⁻¹ are common, but usually for only limited wavelength ranges.

Thus, another primary requirement for an efficient organic photovoltaic material is a broad distribution of high absorption coefficient values. In the case of terrestrial solar cell applications, this absorption spectrum should, if possible, match the average solar spectral radiance as it reaches the earth's surface (AM2 in Fig. 3).

In summary, the necessary properties for a potentially efficient organic photovoltaic material include

- high quantum efficiency for charge generation (by sunlight);
- large absorption coefficients over as broad a range of photon energies as possible (ideally, the absorption spectrum should match the sun's spectral radiation);
- · ready availability from low cost sources;
- good electronic transport properties, such as high mobility and low bulk resistivity;
- high ratio of photocurrent to dark current;
- potential for high barrier heights (using common electrode materials), leading to high voltage outputs;
- capability for easy device fabrication, preferably in thin-film form by solution-casting techniques;
- good performance at high light intensities (90-140 mW/ cm²); and
- long-term thermal, chemical, and electrical stability.

With these basic requirements in mind, two organic photoconductive dye systems were chosen for study as potential solar cell materials.

• Squarylium dyes

A class of organic photoconductive dyes derived from squaric acid and its derivatives [24, 25] are known to have very high extinction (solution absorption) coefficients and

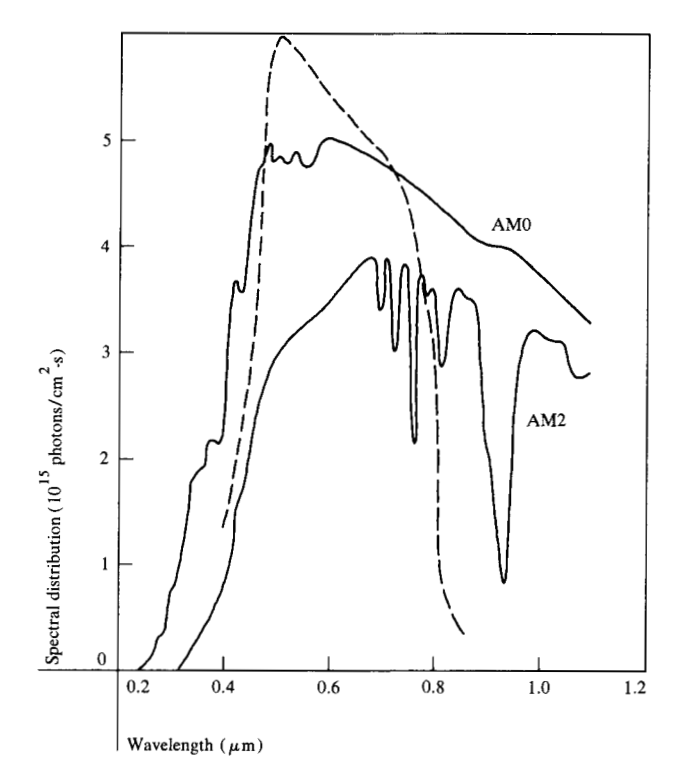


Figure 3 Photon distribution of sunlight under outer space conditions (AM0), and as it reaches the earth's surface under average weather conditions (AM2). These curves were supplied by H. J. Hovel; see [15(b)]. The dashed line represents the solid state absorption spectrum of an amorphous OHSq film.

solution phase absorption maxima over a broad range of visible wavelengths. Some of these dyes can also be vacuum-sublimed (or evaporated) without decomposition; polycrystalline thin films of methyl squarylium (MeSq, structure 5a), hydroxy squarylium (OHSq, 5b), and diethyl OHSq, 5c) have been made in this fashion. The absorption spectra of these solid films are extremely broad,

$$R = R' = CH_3$$
 (5a)

$$R = CH_3$$
, $R' = OH$ (5b)

$$R = C_0 H_E$$
, $R' = OH$ (5c)

but it was felt that further expansion of this absorption might be possible in a close-packed amorphous or glassy state. Such structurally dependent absorption broadening has been observed in other organic systems, such as phthalocyanine [12, 26], and is also well known in the case of aggregated photosensitizing dyes.

357

Since grain boundaries in polycrystalline materials can serve as recombination sites, an amorphous or glassy system might also lead to improved electronic transport properties.

Finally, the possibility exists for forming glassy solid solutions; dyes having different absorption characteristics could then be homogeneously mixed to give a single amorphous or glassy film having a total absorption spectrum extending from ultraviolet to infrared frequencies. One would like to be able to "tailor" any desired absorption by the proper choice of the type and proportions of constituents in the solid solution.

• Cyanine-tetracyanoquinodimethide (TCNQ) salts Another class of photosensitive dyes that exhibit strong absorption in the visible and near-infrared wavelengths

consists of the cyanine dyes (for example, structures 6a and 6b). Most of these are commercially available as iodide salts, and the iodine is easily exchanged in a metathetical reaction with Li⁺TCNQ⁻ to form simple 1:1

$$(\text{or } TCNQ^{-})I^{-}C_{2}H_{5} \qquad (6a)$$

cyanine-TCNQ salts [23, 27-29]. These simple salts can be further reacted (or doped) with neutral TCNQ to form complex salts (or mixed-valence states) similar to those of (TTF)(TCNQ), thus providing organic materials with the potential for higher bulk conductivities. It is expected that the electronic transport properties of these TCNQ salts will be improved over those of the iodide salts. Although dark conductivities are also expected to increase, the ratios of the photo-to-dark current may remain very large; if so, one expects to see enhanced photo-voltaic responses.

If these materials can be made into thin amorphous or glassy films, and if the desirable absorption properties of the original dyes are preserved or enhanced, these salts also represent good candidates for broad-range-absorption solid solutions that could be utilized in possible photovoltaic applications. Many cyanine dyes are known to have p-type conductivity, but it was uncertain whether the particular systems studied would give photovoltages. It was decided that if glassy films having desirable absorption properties could be made, the films would be tested for photovoltaic activity in the same fashion as the squarylium dyes.

Preparation and absorption properties of squarylium films

• Sublimation techniques for MeSq, OHSq, and diethyl OHSq

A special high-vacuum sublimation system was designed to be capable of sustaining an internal pressure of 10⁻⁶ Pa $(\approx 10^{-8} \text{ torr})$. The glass sublimator contained a built-in condenser that could be filled with the desired coolant (dry ice/acetone or liquid nitrogen) for rapid condensation of the vapor phase. The condenser was in contact with a gold-plated copper substrate holder such that the substrate temperature could be maintained at or near the coolant temperature (this could be monitored by a thermocouple). The base of the unit was generally submerged in a preheated, thermostatically-controlled oil bath in order to rapidly initiate the sublimation or evaporation. The dye powders were evenly and thinly dispersed across the entire bottom of the unit and then "caked" with diethyl ether. This dispersion method was critical to the successful sublimation of amorphous films since bulk heating of the dyes, especially OHSq, led to partial decomposition. The source-to-substrate distance was approximately 20 cm. The dye films were evaporated onto 2.5-cm specially cleaned quartz disks, precoated with either transparent In-O (Nesa glass) or Sn-In-O or semitransparent metal films. The average deposition conditions for amorphous films were MeSq—bath temperature, 463-493 K, internal pressure, 10^{-2} - 10^{-3} Pa, dry-ice/acetone or liquid nitrogen coolant; OHSq-463-513 K, 10^{-3} -10⁻⁴ Pa, liquid nitrogen. Film compositions were verified by solution absorption spectra of dissolved films, and by powder x-ray diffraction spectra of scrapings from the films.

The substrate temperature and the internal pressure affect the phase and degree of crystallinity of the films, as determined by scanning electron microscopy (SEM), x-ray diffraction [30], and absorption spectroscopy. For example, three different film phases (blue, purple, or green) were obtained for MeSq by varying the condensate from dry-ice/acetone to liquid nitrogen. The best amorphous OHSq films were obtained with liquid nitrogen; the only evidence for any type of long-range ordering in these films was a possible sheeting. The substrate material and morphology affected the crystallinity of the films, much as has been observed in organic epitaxy [31]. The absorption properties are discussed at the end of this section.

Film thicknesses of approximately 5–1000 nm could be made in this fashion, although the films used for photovoltaic studies were generally 20–200 nm thick (as measured by interferometry).

Solution-casting techniques for OHSq

Up to five weight-percent of those squarylium dyes containing hydroxy substitution in the aromatic ring (struc-

tures 5b, 5c) could be slowly "dissolved" (or complexed in some manner) when n-propylamine or a mixture of propylamine and ethylene diamine was used as the solvent [32]. Absorption spectra of these solutions failed to show the normal squarylium peaks, e.g., $\lambda_{max} \approx 630$ nm in CHCl₃ (the solutions were straw-colored). No evidence could be found for a charge-transfer band (by scanning from 350-2500 nm). The typical dye solution absorption band could be regenerated by adding neutral solvents, such as hexane, to the amine-dye solution. The amine-dye solution may represent a fairly stable and reversible oxidized or protonated form of the dye [33]. However, other amine solvents with similar basicities (pK) failed to "dissolve" the dye or caused decomposition. A thorough discussion of the exact state of the squarylium dye is beyond the scope of this paper.

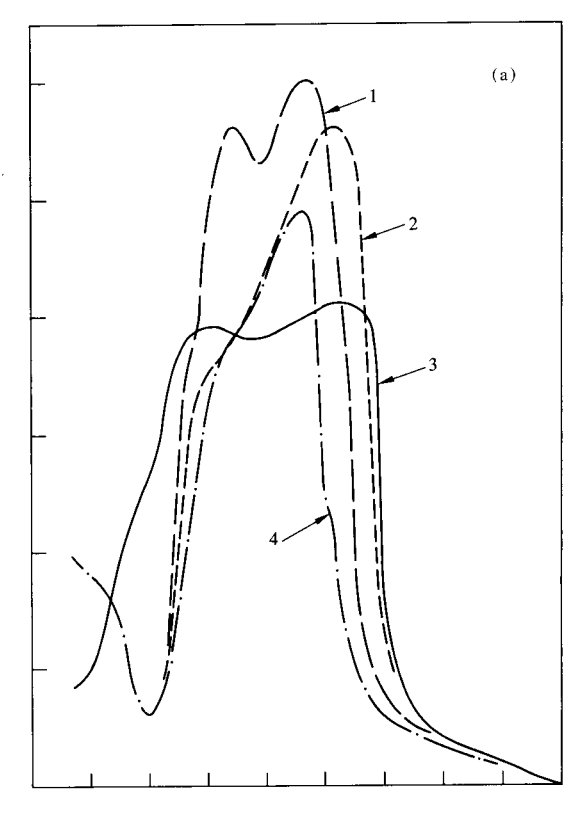
The amine solutions were highly sensitive to light; however, they could be stored for weeks under nitrogen. The photovoltaic properties of cast films remained constant for up to several days if the solutions were simply stoppered.

These solutions were spin-coated onto cleaned substrates, and the volatile solvent was removed (indicated by the absence of amine odor) by a final heat or vacuum treatment. In this way, uniform, highly absorbant, and highly reflective (brassy greenish tinge) films could be obtained that appeared deep purple under transmitted light. The solid state absorption spectra were nearly the same as those of the amorphous sublimed films. As with the sublimed films, the chemical compositions were verified by solution-absorption and x-ray diffraction spectra.

The degree of crystallinity as well as the absorption properties of the films could be varied by using different solvent additives or by post-spin heat or vacuum treatments [see Fig. 4(b)]. The films were completely amorphous (by SEM) when 0-20% ethylene diamine (EDA) in propylamine was used as the solvent. Polycrystalline films were obtained when co-solvents [such as tetrahydrofuran (THF) or dimethylformamide (DMF)] were used, when more than 20% EDA was used, or when the substrates were heated above 423 K. Crystallinity could not be avoided in films thicker than 500-1000 nm, or in those films coated from solutions more concentrated than 5% solids. Film thicknesses averaged between 60 and 80 nm, as determined from the solid state absorption spectra (assuming α values for the sublimed state), and from interferometry on selected films. The films remained amorphous for long periods of time, even when not protected from the atmosphere.

• Absorption properties of squarylium films

The absorption spectra of various sublimed and solutioncast squarylium films are shown in Fig. 4(a). The solid state absorption properties of amorphous films were su-



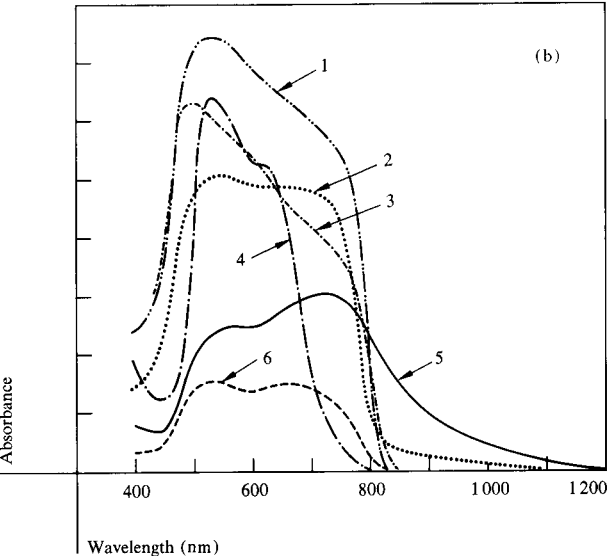


Figure 4 (a) Solid state absorption characteristics of amorphous films of evaporated (1) MeSq, (2) OHSq, and solution-cast (3) OHSq and (4) diethyl OHSq; (b) variations of absorption properties of solution-cast OHSq films with preparation conditions: (1) heat-treated 1:5 EDA/PA, (2) unheated PA, (3) heat-treated PA, (4) unheated 1:5 EDA/PA, (5) unheated polycrystalline EDA, and (6) heat-treated polycrystalline EDA. The curves have been arbitrarily scaled for ease of shape comparison.

perior to those of similar polycrystalline films. Some of the enhanced absorption may also be due to various randomly aggregated species, which on the whole have no

Table 1 Cyanine dye-TCNQ salts and their absorption properties.

Cyanine dye (structure number; see text)	Crystallizing solvent	$\lambda_{\max}(nm); extinction coefficient \ (l-mol^{-1}\text{-cm}^{-1}), \ CH_2Cl_2 \ solvent$
Cyanine (6a, $n = 0$)	Cold EtOH	530; 2.57 × 10 ⁴ 495; 1.60 × 10 ⁴
Dicarbothiacyanine (6b, $n = 1$, $X = S$)	CH_2Cl_2	$660; 1.21 \times 10^{5} \\ 613; 2.72 \times 10^{4}$
Oxadicarbocyanine (6b, $n = 1$, $X = O$)	EtOH	$582; 1.72 \times 10^{5}$ $550; 5.65 \times 10^{4}$
Dicarbocyanine (6a, $n = 1$)	CH ₂ Cl ₂ /MeOH	$717; 2.13 \times 10^{5}$ $657; 6.53 \times 10^{4}$
Tricarbothiacyanine (6b, $n = 2$, $X = S$)	Hot CH_3CN , CH_2Cl_2 , or $EtOH$	$775; 2.62 \times 10^{5} $ $715; 7.12 \times 10^{4}$

uniform "structure." In the case of the amorphous OHSq, the absorption coefficients averaged approximately 10⁵ cm⁻¹ over the entire visible range, and, in fact, nearly matched the AM2 spectrum (see Fig. 3). Reflection losses were considered since the absorption properties of these films are affected by surface reflectivity, which is in turn affected by the degree of crystallinity. The absorption spectra could also be influenced by heat or vacuum treatments, by the particular solvent composition, and by the addition of dopants; see Fig. 4(b). Films of amorphous OHSq were so smooth and uniform that their surface reflectances were as high as 0.7, usually peaking in the 750-850-nm region. In traditional inorganic solar cells an antireflective coating is generally used; thus, it should be remembered that all photovoltaic results presented in this paper are for organic systems in the absence of any such special coatings. Ironically, the backwall configuration, where light is incident through the "ohmic" electrode, actually provided a minor antireflective effect in the case of the In-O substrates; i.e., the total absorbance (1 - R -T) of the cell was larger when measured through the In-O substrate than through the dye film on the substrate because of a slight decrease of surface reflectance in the former case.

Preparation and absorption properties of cyanine-TCNQ films

Five cyanine dyes were exchanged with Li-TCNQ [23, 27–29] by refluxing equimolar amounts in acetonitrile. The 1:1 TCNQ salts either precipitated out of the hot solutions or could be crystallized out by the addition of another solvent. The solution absorption data for these salts are listed in Table 1. The spectra were essentially the same (with only minor absorption shifts) as the original iodide salts. The chemical compositions were verified by

combustion analyses. Resistivity measurements (four-point probe) on 1:1 films gave values of $1.2-2.1 \times 10^4$ ohm-cm; for similar films doped with neutral TCNQ, the resistivities decreased to $4.5-30 \times 10^2$ ohm-cm.

■ Solution-casting techniques

The 1:1 cyanine-TCNQ salts were dissolved in hot, 99.9% purity DMF (Burdick and Jackson Laboratories, Inc., Muskegon, Michigan) to which small amounts of nitrobenzene had been added for viscosity considerations. The weight-percent of solids ranged from one to six. These solutions were spin-coated onto warmed substrates, which were then flash-heated to remove solvent, and then vacuum-cured.

The smooth, highly reflecting films were amorphous, as observed by scanning electron microscopy and electron diffraction. As with the squarylium films, the only "structure" detectable was some possible sheeting. When cosolvents such as THF were used, even in trace amounts, polycrystalline films were obtained. In addition, the films were amorphous only for thicknesses up to about 20 nm; attempts to increase the film thickness by increasing either the solids content or the viscosity of the casting solution, or by decreasing the spinning rate, resulted in polycrystalline films. Many of the films tended to crystallize on standing, whereas others remained amorphous for months.

It was possible to cast thin amorphous films of solid solutions of the two salts oxadicarbocyanine-TCNQ (denoted ODC-TCNQ, structure 6b, n=1, X=0) and diethyldicarbocyanine-TCNQ (DC-TCNQ, 6a, n=1). The 1:1 mixture was made by casting a hot solution of ODC-TCNQ (3.44 mg) and DC-TCNQ (3.47 mg) in DMF (0.4 ml). The 1:2 mixture used 2.00-mg, 4.15-mg, and 0.4-ml quantities, respectively.

• Absorption properties of cyanine-TCNQ films

Although very broad absorption was obtained for the amorphous films, the absolute absorbance of these films was never greater than approximately 0.7 [see Fig. 5(a)]. Films that crystallized lost the desirable broad absorption and appeared transparent except for small flecks of solid material. Films of the amorphous solid solutions gave spectra attributable to additive absorption of the pure components [Fig. 5(b)].

Experimental conditions for electrical measurements

The light source for initial experiments was a He/Ne laser (632.8 nm), a Bausch & Lomb high intensity (100 mW/cm²) white light, or a filtered 1-kW xenon lamp simulating the AM0 solar spectrum (see Fig. 3). Neutral density filters were used to vary the input intensity, and narrow bandpass filters were used to obtain the spectral response studies.

For most films less than or equal to 70 nm thick, it was difficult to evaporate semitransparent and continuously conductive top electrodes without shorting the devices; therefore, liquid gallium or mercury was generally used as the top Schottky barrier electrode, and the light was incident on the "ohmic" substrate, i.e., a backwall cell. (In a frontwall cell, the light is incident on the Schottky barrier electrode. With film thicknesses greater than W+L, the frontwall configuration is preferred since one can better utilize the superior absorption properties of the films by generating most of the carriers near the active electrode.)

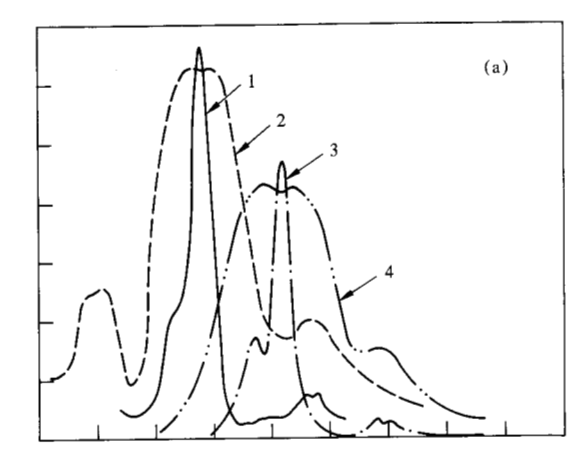
All of the films tested behaved as p-type semiconductors; the photocurrents measured at the top Schottky electrode were negative in polarity. Photovoltaic measurements were taken in the standard fashion with appropriate shielding. In these studies no effort was made to protect the devices from the ambient atmosphere.

Experimental results

• Dark current-voltage curves

The dark electrical characteristics of the organic thin-film devices generally exhibited rectifying behavior, the rectification ratio being a function of the electrode material and the organic film thickness. Figure 6 shows typical dark current-voltage (*I-V*) curves for sublimed films (40–100 nm thick) of OHSq on both In-O- and Pt-coated quartz substrates. Devices containing MeSq, diethyl OHSq, and the cyanine-TCNQ films showed similar behavior; the rectification ratios tended to be smaller and the curves tended to appear as in trace 1.

Many of the cyanine-TCNQ devices either gave no photovoltage at all or shorted out, possibly due to the thinness of the films. None of the undoped squarylium films had measurable dark voltages; however, some of the



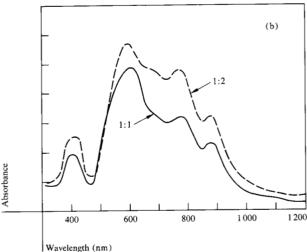


Figure 5 (a) Solid state and solution absorption spectra for cyanine-TCNQ films: (1) oxadicarbocyanine-TCNQ solution; (2) solid state; (3) dicarbocyanine-TCNQ solution; (4) solid state. (b) Solid state absorption spectra for solid-solution films: 1:1 (solid line) and 1:2 (dashed line) oxadicarbocyanine-TCNQ and dicarbocyanine-TCNQ. The curves have been arbitrarily scaled for shape comparisons.

cyanine-TCNQ films and the heavily doped squarylium films had dark voltages as high as 0.2 V; these were always subtracted from all reported photovoltage values.

• Spectral response

Due to the inferior behavior of the MeSq, diethyl OHSq, and cyanine-TCNQ films, the spectral response (absolute quantum efficiency as a function of wavelength of incident light) was studied only for the OHSq films, and only for sublimed films on both In-O and Pt electrodes. The spectral response of these cells was typically broad. In cases where the film thicknesses were greater than approximately 35 nm for In-O, or approximately 45 nm for Pt, the spectral response resembled the inverse of the absorption spectrum (see, for example, Fig. 7). If the film

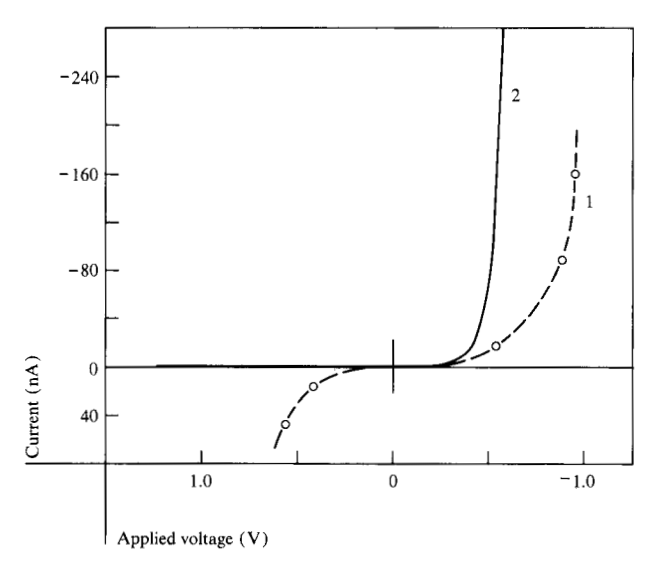


Figure 6 Dark current-voltage behavior of typical evaporated OHSq films: (1) Ga/42-nm OHSq/ln-O cell; (2) Ga/56-nm OHSq/Pt cell. The photocurrents measured at the Schottky electrode (Ga) are negative in polarity.

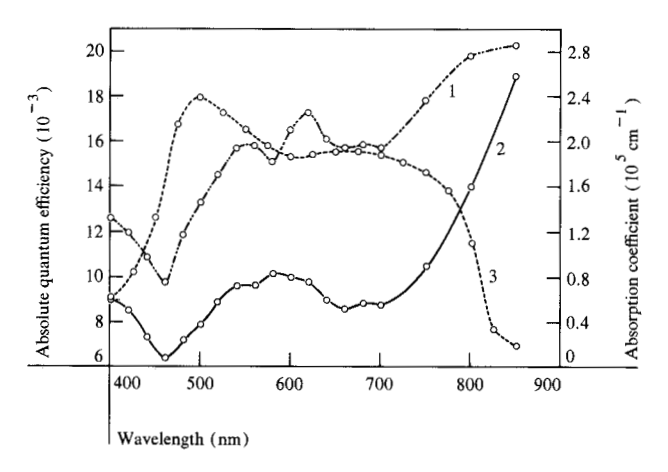


Figure 7 Response spectra for evaporated OHSq films in comparison with absorption spectrum (curve 3): (1) Ga/42-nm OHSq/In-O; (2) Ga/56-nm OHSq/Pt.

Table 2 Short-circuit currents of OHSq cells as a function of film thickness; an estimate of the optimum cell thickness.

Cell	Thickness (nm)	$J_{\rm sc} \ ({ m mA/cm^2})$
Ga/In-O	10	0.18
	45	0.58
	90	0.01
Ga/Pt	60	0.80
	90	1.24
	130	0.72

Table 3 Comparison of open-circuit voltages of similar Ga/Pt and Ga/In-O devices measured with AM0 light.

	Open-circuit voltages (V)			
Intensity (mW/cm ²)	Ga/Pt	Ga/In-O		
0.10	0.39-0.46	0.37		
5	0.51	0.37		
90	0.66	0.55		
135	0.66	0.55, 0.64		

thicknesses were less than the limits mentioned above, the spectral response matched the absorption spectrum. The highest quantum efficiency observed (uncorrected for electrode absorption) was 0.023 at 850 nm for a Ga/40-nm OHSq/In-O cell. Quantum efficiencies decreased with increasing film thickness and were higher for amorphous (as opposed to polycrystalline) films.

• Photovoltaic measurements on evaporated MeSq films Only homogeneous amorphous blue films (65–97 nm thick) prepared by dry-ice/acetone condensation were tested with 21-mW/cm² white light. The substrate electrodes included Sn-In-O, In-O, Cr, and W. The maximum conversion efficiency, 0.002% (uncorrected for electrode absorption), and short-circuit current density $J_{\rm sc}$, 4 μ A/cm², were measured for a Ga/Cr cell. A Ga/In-O device gave the best open-circuit voltage, 0.57 V. The fill factors were all poor (0.25), and, in general, η values were only about 10^{-4} percent.

Photovoltaic measurements on undoped, evaporated OHSq films

The photovoltaic properties of these devices were tested as functions of film thickness, electrode couple, light source, polycrystallinity (or lack of it), and light intensity. The effects of intensity are discussed in a separate section.

Film thickness Generally, for amorphous films less than 100 nm thick, the efficiences were consistently between 0.01 and 0.06%; for films 100–300 nm thick, η ranged from 10^{-3} to 10^{-2} percent; for films as thick as 600 nm, η dropped to $0.8-5.2 \times 10^{-4}$ percent.

Changes in $V_{\rm oc}$ with film thickness were negligible; however, as would be expected, $I_{\rm sc}$ was dependent on film thickness. Plots of $I_{\rm sc}$ vs thickness showed maxima at approximately 45 nm for Ga/In-O cells, and at about 90 nm for Ga/Pt cells (see Table 2). The highest $J_{\rm sc}$ measured was 2.0 mA/cm² (135 mW/cm², AM0) for a 50-nm Ga/Pt cell with a 0.02% efficiency.

Table 4 Photovoltaic parameters for best evaporated OHSq Schottky barrier devices for different light sources.

Light source	Intensity (mW/cm²)	Electrodes	Film thickness (nm)	$rac{V_{ m oc}}{ m (V)}$	$J_{ m sc} \ (\mu ext{A/cm}^2)$	FF	η (%)
850 nm	1	Ga/In-O	42	0.58	13	0.27	0.20
633 nm	94	Ga/In-O	30	0.54	350	0.27	0.054
White	21	Ga/Sn-In-O	70	0.58	78	0.27	0.058
	9.6	Ga/In-O	85	0.54	37	0.27	0.052
AM0	0.14	Ga/In-O	42	0.46	1.5	0.20	0.10
		Ga/Pt	56	0.46	1.2	0.37	0.15
	134, 135	Ga/In-O	40, 42	0.55, 0.64	240, 115	0.20, 0.19	0.02, 0.01
	,	Ga/Pt	56, 60	0.66	150, 195	0.27, 0.21	0.02

Electrodes The most extensive electrode comparison tests were between Ga/In-O and Ga/Pt, but other electrode couples studied included Ga/Sn-In-O, Ga/Cr, and Hg/Cr.

The highest $V_{\rm oc}$ values (0.66 V) at comparable intensities were observed for Ga/Pt devices. See Table 3 for steady state open-circuit voltages for Ga/Pt and Ga/In-O devices tested with AM0 light. The lowest open-circuit voltages were observed for Ga/Cr and Hg/Cr electrodes (0.43–0.49 V at 135 mW/cm².

Comparisons of Sn-In-O and In-O devices showed similar $V_{\rm oc}$ values, but the lower-sheet-resistivity Sn-In-O often gave higher short-circuit current densities.

The fill factors were consistently higher for Ga/Pt cells (0.21–0.40), and at times as much as twice those for Ga/In-O devices (0.19–0.31). Figure 8 shows photocurrent-voltage curves for two typical Ga/Pt and Ga/In-O cells [12].

Light source Four different light sources were used: 633-nm He/Ne laser, 850-nm Xe, white light, and AM0 simulated light. The best photovoltaic parameters obtained for each light source (high and low intensity) are listed in Table 4.

Crystallinity In every case where devices of amorphous and polycrystalline films of similar thicknesses were tested under identical conditions, the amorphous devices gave conversion efficiencies an order of magnitude or more higher than their polycrystalline counterparts. Since the $V_{\rm oc}$ were essentially the same, these efficiency increases were due primarily to corresponding increases in $I_{\rm sc}$, but also sometimes to increases in FF. Table 5 illustrates these effects for a pair of Ga/230-nm OHSq (0.25-cm²)/In-O cells tested with 21-mW/cm² white light.

Photovoltaic measurements on undoped, solution-cast OHSq films

The photovoltaic parameters were studied as functions of the electrode couple and of the sheet resistivity of the bot-

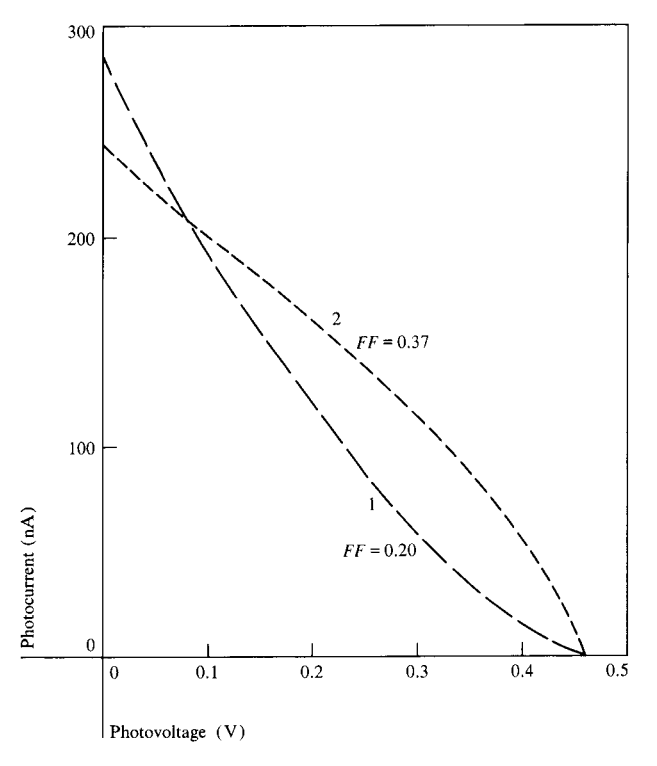


Figure 8 Steady state illuminated photovoltaic *I-V* curves for (1) Ga/42-nm OHSq/In-O; (2) Ga/56-nm OHSq/Pt cells, AM0 light, 0.14 mW/cm². Note that the fill factor for the Pt cell is nearly double that for the In-O cell.

Table 5 Comparison of photovoltaic parameters for amorphous and polycrystalline Ga/230-nm OHSq/In-O cells.

Film type	$rac{V_{ m oc}}{({ m V})}$	$J_{ m sc} \ (\mu { m A/cm^2})$	FF	η (%)
Amorphous	0.52	20	0.27	$1.3 \times 10^{-3} \\ 7.5 \times 10^{-5}$
Polycrystalline	0.53	1.2	0.25	

Table 6 Photovoltaic parameters for solution-cast OHSq films sandwiched between various metallic electrodes.

Electrodes	Transmission of bottom electrode (%)	Intensity (mW/cm²)	$V_{ m oc} \ ({ m V})$	$J_{ m sc} \ (\mu { m A/cm^2})$	FF	$\eta_{ m corr} \ (\%)$
Ga/Pt	4.75	0.24	0.47	19	0.412	0.32
Ga/Pt	43	0.24	0.52	19	0.336	0.032
Ga/Au ^a	51	0.94	0.52	0.11	0.332	4.0×10^{-4}
Ga/Ni ^a	30	0.41	0.38	0.6	0.336	6.2×10^{-4}
Ga/Ag	63	0.94	0.38	38	0.300	0.007
Hg/Pt	4.75	0.41	0.38	10	0.412	0.080
Hg/Au	51	0.94	0.51	30	0.332	0.011
Hg/Ni ^a	30	0.41	0.35	1.4	0.336	0.001

aPolycrystalline.

 Table 7
 Transmission and sheet resistivity values for In-O and Pt-coated substrates.

Substrate	Transmission (%)	Sheet resistivity (ohm-cm)
In-O	95	191, 175
Pt (5 to 10 nm)/quartz	35	155
•	40	262
Pt (3.5 nm)/Bi ₂ O ₃ (10 nm)	49	155
Pt (3.5 mn)/In-O	43	76,82
•	45	78
	47	95

tom collecting electrode. The maximum (uncorrected for electrode absorption) power conversion efficiencies measured for nonhybrid electrode devices were 0.063% (for both Hg/In-O and Ga/In-O; $V_{\rm oc}=0.28~{\rm V},\,J_{\rm sc}=0.75~{\rm mA/m}$ cm^2 , FF = 0.27) with the 90-mW/cm² white light, and 0.024% (Ga/In-O; $V_{\text{oc}} = 0.52$, $J_{\text{sc}} = 0.13 \text{ mA/cm}^2$, FF =0.27) with 0.76-mW/cm², 633-nm He/Ne laser light. Of the hybrid-electrode devices (tested with the He/Ne laser), the maximum uncorrected efficiency was 0.042% (Ga/ Pt,In-O). If corrections are made for electrode absorbance, the maximum efficiencies $\eta_{\rm corr}$ were 0.32% [Ga/Pt (4.75% transmittance)], 0.086% [Ga/Pt,In-O (47%)], and 0.08% [Hg/Pt (4.75%)]. It should be stressed, however, that these η_{corr} cannot be achieved with real working devices; the values are useful only for making theoretical comparisons among the various electrode systems. Table 6 lists the photovoltaic parameters of solution-cast OHSq films sandwiched between various nonhybrid metallic electrode couples; these devices were tested with the He/Ne laser. The best electrode systems are Ga/Pt and Hg/Pt. Generally, although the $V_{\rm oc}$ for solution-cast OHSq films were lower than those obtained for evaporated films, the short-circuit currents and fill factors were higher.

The measured sheet resistivities and the corresponding transmittance values for In-O, Pt on quartz, Pt on $\mathrm{Bi_2O_3}$, and Pt on In-O films are shown in Table 7, and the photovoltaic parameters of solution-cast OHSq cells made from these electrodes are shown in Table 8. It is clear that the hybrid Pt,In-O device gives the highest corrected (0.086%) or uncorrected (0.042%) efficiencies.

The thicknesses of these films ranged from approximately 25 to 90 nm.

Solution-cast cyanine-TCNQ salts Although extensive studies have not been made on these dye systems, power conversion efficiencies as high as 0.02% were measured for thin films on In-O, with the same He/Ne laser source mentioned previously; the best device was a Ga/dicarbocyanine-TCNQ/In-O cell. The photovoltaic parameters for three successfully tested cyanine dye systems are shown in Table 9.

The open-circuit voltages were generally much lower than those obtained for OHSq (0.12-0.45 V), but the short-circuit currents were quite respectable when one considers the much lower film absorbances.

Two solid solutions of dicarbocyanine-TCNQ and oxadicarbocyanine-TCNQ (1:1 and 1:2) were also successfully tested (see Table 9). The open-circuit photovoltages were intermediate between those obtained for the pure components, whereas the short-circuit currents were about the same.

Dependence of photovoltaic behavior on input light intensity

This dependence was studied extensively only in the case of OHSq cells. The values of the open-circuit voltage, the short-circuit current density, the fill factor, and the power conversion efficiency were all dependent upon the incident power intensity L. For 100-mW/cm^2 incident intensity of AM0 sunlight, $V_{\rm oc}$ and $I_{\rm sc}$ both tended to decrease slowly with time to steady state values about five percent lower for Pt-coated substrates, and 20 percent

Table 8 Comparison of photovoltaic devices of solution-cast OHSq on Pt, In-O, and hybrid Pt electrodes.

Electrodes	Electrode transmission (%)	$V_{ m oc} \ m (V)$	Intensity (mW/cm²)	$J_{ m sc} \ (\mu ext{A/cm}^2)$	FF	η (%)	η _{согг} (%)
Ga/Pt	43	0.52	0.24	19	0.34	0.014	0.032
Ga/Pt,Bi ₂ O ₃	49	0.42	0.68	33	0.30	0.006	0.012
Ga/Pt,In-O	47	0.38	0.68	210	0.36	0.042	0.086
Ga/In-O	_	0.41	0.68	110	0.27	0.018	0.018

Table 9 Photovoltaic results on cyanine-TCNQ simple salts; Ga/In-O electrodes, He/Ne 933-nm light of 0.94 mW/cm² intensity; FF = 0.30, 1.5% solids loading in solution unless noted otherwise.

Cyanine dye	Structure number (in text)	Solventa	$V_{ m oc} \ ({ m V})$	$J_{ m sc} \ (\mu m A/cm^2)$	Conversion efficiency (10 ⁻³ %)
Oxadicarbo	6b, $n = 1$, $X = O$	DMF DMF/C ₆ H ₅ NO ₂	0.45 0.32	30 44	4.3 4.5
Dicarbothio	6b, $n = 1, X = S$	DMF	0.27	190	17.0
Dicarbo	6a, n = 1	DMF	0.12	70	2.7
1:1 dicarbo/oxadicarbo		DMF	0.17	46	2.5
(1.75% solids) 2:1 dicarbo/ oxadicarbo		DMF	0.29	15	1.3

^{*1.5%} solids in DMF gives films approximately 50 nm thick; in DMF/C₆H₅NO₂, approximately 60 nm.

lower for In-O-coated substrates, as compared to the instantaneous values (the moment light is applied). For example, for a 56-nm Ga/Pt cell the initial $V_{\rm oc}$ was 0.656 V and decreased to a steady state value of 0.640 V; for a 42-nm Ga/In-O cell the initial $V_{\rm oc}$ was 0.553 V and decreased to 0.434 V at steady state. This slow decrease is less at smaller input intensities and disappears below about 5 mW/cm².

The values for η , $J_{\rm se}$, $V_{\rm oc}$, and FF as a function of input intensity (AM0 light) are shown in Fig. 9 for a typical sublimed 89-nm OHSq film on Pt. The measured short-circuit currents vary linearly with the input intensity L:

$$J_{\rm sc} \propto L^n, \qquad n = 0.8-1.0,$$
 (7)

where n = 0.8 for some In-O cells, but is 1.0 for most In-O and the Pt cells. The open-circuit voltage varies as the log of the intensity. The fill factor was relatively constant at low intensities, but decreased at higher intensities. The power conversion efficiency, following the relationship in Eq. (1), generally peaked in the 0.5-5.0-mW/cm² input power range and then decreased at higher intensities.

Doping experiments

■ Bromine

Preliminary experiments on a sublimed OHSq cell (32 nm, Ga/In-O) with bromine vapor as the dopant, in-

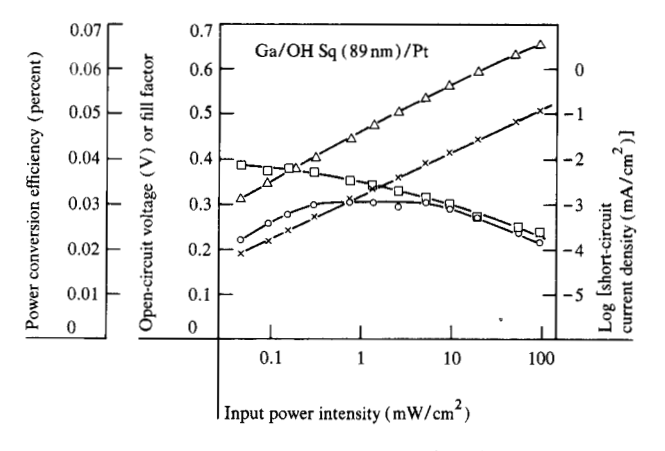


Figure 9 Photovoltaic parameters as a function of light intensity for Ga/89-nm OHSq/Pt: △ open-circuit voltage; □ fill factor; ○ power conversion efficiency; × short-circuit current density (right-hand scale).

creased the 633-nm (94-mW/cm²) conversion efficiency (0.048%) of the undoped cell by a factor of five, to 0.23%; however, the improved efficiency degraded slowly with time. The absorption of the bromine-doped film was considerably lower than that of the undoped film (by a factor of five to ten), yet the efficiency still increased fivefold. It was also observed that the Ga electrode appeared to wet. The doped films, on standing overnight under am-

bient atmospheric conditions, reverted to their original form, and original absorption and photovoltaic values were observed. Another less efficient cell (approximately 600 nm thick, Ga/Sn-In-O) that was lightly doped with bromine vapor also gave an approximate fivefold increase in efficiency (0.82 to 3.7×10^{-4} percent) when 94-mW/cm² white light was used; other photovoltaic parameters are listed in Table 10. In the first example, doping increased the $V_{\rm oc}$, $I_{\rm sc}$, and FF values. In the second example, only the short-circuit current increased by a factor of five. In all cases, if the doping was too heavy the photovoltaic properties were completely degraded; the devices shorted out. Unfortunately, the exact amount of doping was not measurable.

◆ DEASP

Solution-cast films of OHSq were also doped with 1-phenyl-3-p-N,N-diethylaminostyryl-5-p-N,N-diethylaminophenyl- Δ^2 -pyrazoline, denoted as DEASP (structure 8).

$$\begin{array}{c|c} C_2H_5 \\ C_2H_5 \\ C_2H_5 \end{array}$$

This and similar pyrazolines have been investigated as hole transport materials in photocopier applications (see for example [34]), and many can be cast as amorphous or glassy films.

The DEASP was added to the original casting solutions in varying amounts. For films with up to 0.05 weight-percent DEASP (tested in Ga/In-O mode), the conversion efficiencies increased approximately fivefold (e.g., 0.004-0.021%; also, see Table 10), while at the same time the film absorption decreased slightly. These efficiencies did not degrade with time. When larger percentages of DEASP were added, the photovoltaic properties of the films degraded.

Discussion

♦ Conditions of film preparation

The conditions used for the preparation of films were designed to enhance the probability of obtaining the amorphous phase. These conditions, in the sublimation process, involved extremely rapid condensation of the vapor phase by means of liquid nitrogen or dry-ice/acetone cooled substrates. Flash evaporation techniques (and higher bath temperatures), which increase the vaporphase concentration, are expected to favor the amorphous phase; however, under such conditions, vapor phase decomposition of the dyes was detected. The

high vacuum system allowed the vapor phase concentrations to be increased without excessive heating.

In the solution process, the unique amine solvent had a twofold purpose. First, it allowed substantially increased concentrations (1.5%) of squarylium dyes to be "dissolved" and subsequently cast. For example, solution in hot DMF is limited to about 0.015 percent solids content. The high concentrations are required for the casting of thicker, highly absorptive, and amorphous or glassy films. This is similar in principle to the increased vapor phase concentrations in the sublimation process. The amine solvents may serve as weak binding agents (but recall that a full charge transfer complex could not be detected) or as aggregating nuclei. It also appears that both strong basicity and small solvent size are important to the "solution" process since other amine solvents with similar pK values but larger size did not enhance the normal solubility (0.015%).

The second important feature of the amine solvent was its high volatility. In both the spin-coating and flash-heating processes, rapid removal of the solvent causes instantaneous solidification and crystallization is repressed. Again, a slightly different version of this method (rapid condensation with liquid nitrogen) was used in the sublimation process, and such techniques increase the probability of obtaining amorphous films.

♦ Enhanced absorption and transport properties of amorphous films

The amorphous squarylium dye films exhibited enhanced absorption properties, as had been predicted in the early part of this paper. The planar molecules can apparently close-pack randomly in a sheetlike fashion, and both evaporated and solution-cast films possess this same type of ordering. There is evidence from small-signal admittance measurements [35] that conductivity in the amorphous films involves a hopping mechanism, a tunneling mechanism, or a combination of these, and if so, it is likely that the intermolecular or intersheet spacings are on the order of tenths of nanometers. There may be extensive but random orbital overlap between the π systems of different phenyl rings or between phenyl rings and nonbonding orbitals on oxygen or nitrogen in the close-packed amorphous state. Such mechanisms could enhance the charge transport properties of amorphous films; the mobilities [36] are very likely increased over those of polycrystalline films where grain boundaries can serve as effective trapping and recombination sites. In all cases where the photovoltaic properties of otherwise similar polycrystalline and amorphous films were compared, the amorphous films were better by at least an order of magnitude, and it was the short-circuit currents that were higher (rather than the open-circuit voltages), implying more efficient charge transport, more efficient charge col-

Table 10 Photovoltaic measurements for undoped/doped OHSq devices; He/Ne light source.

Dopant	Electrodes	Intensity (mW/cm ²)	$V_{ m oc} \ ({ m V})$	$J_{ m sc} \ (\mu { m A/cm^2})$	FF	$^{\eta}_{(\%)}$
None)	C / C	0.07	0.20	57	0.30	0.004
DEASP	Ga/In-O	0.86	0.42	140	0.30	0.021
None	0.7	0.4	0.51	330	0.27	0.048
Bromine	Ga/In-O	94	0.59	790	0.46	0.23
None	G 15 T O	0.4	0.52	0.55	0.27	8.2×10^{-5}
Bromine	Ga/Sn-In-O	94	0.52	2.5	0.27	3.7×10^{-4}

lection, decreased trapping effects, or any combination of these.

Even though the absorption properties of the amorphous cyanine-TCNQ films were not as good as had been hoped, the thin films did show evidence of increased conductivity; this would account for the very reasonable $I_{\rm sc}$ values that were obtained despite the decrease in actual carrier concentrations expected because of the poor absorbances of the films.

Comparison of evaporated and solution-cast amorphous OHSq films

Although the conversion efficiencies were essentially the same for both evaporated and solution-cast OHSq films, in most cases this resulted from smaller open-circuit voltages but larger short-circuit currents in the solution-cast devices. The decreased voltages may be due to several factors: surface states that decrease the contact potential between the organic surface and the Schottky barrier electrode; leakage currents or defect mechanisms (e.g., traps, surface channels, pinholes, etc.) within the active region; or dark voltages, which offset the photovoltages. The larger short-circuit currents probably reflect increases in the charge carrier densities or in the conductivity of the films. It is also possible that a more "ohmic" contact may exist in the case of solution-cast films if the solution process leads to more intimate contact between the film and the metal electrode surfaces.

• Doping experiments

The improved response of better conducting films was also demonstrated by the doping experiments with the pyrazoline hole transport material (structure 8). The idea was to disperse the OHSq dye in a conductive glassy matrix in such a way as to preserve the desirable absorption and charge-generation properties of the dyes, but at the same time to increase carrier mobility for better collection efficiencies. These films gave fivefold efficiency increases as long as the intermolecular dye distances were small (low dopant levels of DEASP).

The doping experiments with bromine vapor (an acceptor) had the potential both for enhancing the conductivity of the films by introducing partial charge transfer or mixed-valence states and for providing favorable surface state band-bending that could lead to higher output voltages. The concept of partial charge transfer has been used by many in the study of organic conductors, e.g., [37–40], and in the preparation of conductive polymers, e.g., [41-44]. In fact, polymeric semiconductors (such as Br and BF, salts of polyacetylene [41]), when coupled with favorable absorption, photoconduction, and solution (casting) properties, may well possess the greatest potential for producing photovoltaic materials capable of yielding conversion efficiencies of one percent or more. When OHSq films were doped with small concentrations of bromine vapor, fivefold increases in the conversion efficiencies (e.g., 0.048-0.23%) were measured. Partial oxidation of the films probably occurs at low doping levels, and, in fact, cyclic voltametry has indicated that bromine is capable of generating two dye oxidation states (the first reversible, the second not) [33]. There was also some evidence that the bromine vapor affected the gallium electrode (increased wetting). The increased efficiencies slowly reverted to their original values. Obviously, more thorough and controlled doping studies are necessary in order to establish the identity of the specie(s) and the nature of the mechanisms involved.

Despite the preliminary nature of these doping experiments it is clear that efficiency increases of at least five-fold can be readily obtained. Thus, if 0.1-0.2% efficient cells could be doped, one might expect efficiencies near one percent. It is also likely that a better understanding of the effects of donor-acceptors or other dopants on the squarylium films could give potential efficiency increases (with current technologies) of an order of magnitude or more.

• Intensity dependence of photovoltaic parameters Most organic materials that have been studied in the photovoltaic mode have not been measured at intensities

much above 10-20 mW/cm² because the materials, or their electrical properties in the device configuration, tended to degrade at higher intensities. In addition, the effects of space-charge-limited currents are accentuated at higher intensities because of increased carrier densities, and this generally results in degradation of the photovoltaic properties (decreases in FF and V_{oo}). It should also be remembered that minority-carrier mobility and collection, especially in organic devices, is field-dependent. As the output photovoltage from the cell increases, the internal electric field decreases, causing decreases in the collected currents. These effects can be observed as a decrease in the fill factor with increasing intensity, as a saturation of the photocurrent with increasing intensity, or as time-dependent open-circuit photovoltages and currents.

The performance of OHSq cells at intensities as high as 140 mW/cm² was as good or better than any reported for an undoped organic material at much lower intensities [8-12, 15b]. The short-circuit currents continued to increase linearly with the intensity [n = 1 in Eq. (7)] except in a few of the In-O cells, where n = 0.8.

The improved high intensity performance may also be due in general to decreases in trapping effects.

• Ohmicity of collecting electrode and hybrid electrodes The increased fill factors observed for the Pt devices can result from the increased "ohmicity" of the collecting electrode or from decreased leakage currents caused by defects such as traps, surface channels, pinholes, etc. The structure and purity of the films should be essentially the same since both In-O and Pt substrates were coated (by sublimation) in the same run; therefore, it is most likely that the increased FF values are due to increased "ohmicity." Since no detailed "structure" could be observed in either film, it is not possible to know whether small differences in such factors as intersheet spacing, aggregate size, polarity, micro-orientation, etc. occurred as a result of the different substrate surfaces; these could certainly affect the collection efficiencies. The work function of In-O is between 4.3 and 4.7 eV [21]. Since the work function of thin films of amorphous OHSq similar to those used in the cells studied has been determined to be 4.15-4.20 eV [21], it is possible that a small contact barrier could be present at some of the OHSq/In-O interfaces; the height of such a barrier would depend on the presence of surface states or impurities. In the case of MeSq, where $\phi \approx 4.5 \text{ eV}$, contact barriers of approximately 50 mV were measured. This would explain the poor conversion efficiencies found for the In-O cells (relative to cells with higher work function electrode materials).

The presence of a second contact barrier at the collecting electrode can significantly affect the photovoltaic re-

sults. There are good mathematical treatments of the effects of such double barriers (one at the Schottky electrode and one at the presumably ohmic contact) on the response spectra [10, 11]. The maximum photovoltage (at equilibrium) in these cases is dependent on the difference between the two barrier potentials and on the respective active depths of those barriers since they would tend to offset each other. In addition, there may be a time-dependent steady state voltage, since each of the developing barrier voltages effectively biases the other (recall that the carrier mobilities are field-dependent). A second nonohmic surface can also serve as a trapping or recombination site, and values of the fill factors may decrease. If the second barrier is not significant, the I_{sc} may be only slightly decreased, but the fill factors will probably remain low.

When the high work function Pt electrode ($\phi = 5.6$ -6.0 eV [45] is used as the collecting electrode, this second barrier is removed (or at least decreased considerably). Unfortunately, good semitransparent (>60% transmittance) films of Pt are obtained only for film thicknesses on the order of two to four nanometers. For plain evaporated or sputtered Pt films (on glass) these thicknesses are not sufficient to guarantee complete and homogeneous electrical continuity; the sheet resistivities (100-300 ohm-cm) are thus much higher than bulk Pt values. Continuity occurs reliably for film thicknesses of about 15 nm or more and these films have transmittances usually less than 40-50%. However, platinum films can be sputtered onto Bi₂O₃ [46] to give greater transmittance and continuous electrical properties for very thin Pt layers (3.5-5 nm). It was decided that very thin Pt films would instead be sputtered onto In-O in the hope of deriving continuity from the underlying In-O film, while retaining the characteristically high work function of Pt [47].

The results given in Tables 7 and 8 illustrate the enhanced conductivity properties of the hybrid films. Although devices consisting of solution-cast OHSq on these substrates showed lower open-circuit voltages (possible decreases in contact potentials), both the fill factors and the short-circuit currents were higher; the efficiencies were increased fivefold over similar nonhybrid electrodes.

The alternate electrode systems tested included collecting electrodes of high work function materials such as Au (5.1 eV) and Ni (5.2 eV) and low work function materials such as Ag (4.3-4.6 eV) or W (4.5 eV). The photovoltaic results were generally consistent with predictions from band theory. These systems were never studied in detail because the open-circuit voltages and (especially) the short-circuit current densities were poor compared to those obtained for the In-O and Pt cells.

Attempts were made to create frontwall cells by using Hg/Cr, Hg/Al, or Ga/Al electrodes; however, the photo-

voltaic properties generally suffered considerably and they were not tabulated. In the case of the Al electrodes, extremely erratic results were obtained; dark voltages were often observed, probably due to the presence of oxides on the Al surface. To eliminate these problems a closed-system, multiple-evaporation unit will be used in future studies of these electrode couples.

• Device configuration and response spectra

Ideally, with p-type organic semiconductors, one would like to have a solid, nearly transparent, Schottky barrier (low work function) electrode (e.g., Al/In-O) coupled with an efficient "ohmic" collecting electrode such as the Pt/In-O hybrid electrode; this would permit frontwall cells. If film thicknesses of 45-90 nm are used, the efficiencies should improve because of the higher collection efficiencies for carriers generated near the active electrode. That is, the carriers would not have to travel a long distance (compared to a diffusion length) through high bulk resistivity organic material before reaching a collecting electrode. Even if actual charges are generated not in the bulk but at the electrode surface (exciton mechanisms), the energy transfer (exciton diffusion) would be more efficient since the excitons would encounter fewer traps or other deactivating species.

The behavior of the response spectra of frontwall and backwall cells is directly related to the above discussion. The following greatly simplified discussion of response spectra holds for single-photon carrier generation schemes where carrier transport (mobility and resistivity values) is finite. These assumptions appear to be valid for the undoped squarylium films discussed in this paper. Other generation schemes and transport mechanisms can occur with organic materials. The reader is referred to [15] for more thorough discussions, particularly with respect to excitonic diffusion mechanisms.

The response spectra [quantum efficiency (or sometimes short-circuit current) vs wavelength of exciting light] of backwall cells in which the organic films are thicker than W+L are expected to have a generally inverse dependence on the organic absorption spectra because the films themselves act as light filters. The only wavelengths capable of reaching the deeply situated (with respect to the incident surface) active barrier region are those that are weakly absorbed. The strongly absorbed light creates carriers within film layers outside the active region, and these carriers are not collected before being trapped or recombining.

For backwall cells in which the film thickness is less than or equal to W+L, all light absorption occurs within the active region and there is a direct correlation between the response spectrum and the light absorption. The same statement holds for frontwall cells with any film thickness in which the carriers can be reasonably collected (and de-

tected), since carrier generation is directly dependent upon light absorption.

• Schottky barriers

Clearly, it would be interesting to examine other electrode systems in detail. Some workers have attributed photovoltages observed by them to potential differences between the two electrodes rather than to true Schottky barrier potentials. A detailed study of various electrode couples would help to clarify this point with respect to many organic systems. Studies of the capacitance of the devices as a function of the applied voltage V can help to establish the presence of a true Schottky barrier, since in such cases the capacitance C of the device is a function of the difference between the barrier potential $V_{\rm b}$ and the applied voltage V:

$$\frac{1}{C^2} \propto V_{\rm b} - V. \tag{9}$$

• Efficiency enhancement

There are several known techniques for enhancing conversion efficiencies of photovoltaic devices. Those most likely to be useful in enhancing organic photovoltaic responses are mentioned here.

Grid electrode patterns have been designed to reduce the detrimental effects of high bulk resistivities [48] while increasing the amount of light penetrating the bulk material. These grid patterns might be expected to enhance cell efficiencies perhaps by a factor of two to ten by increasing both photocurrents and fill factors.

Previously, it was mentioned that the amorphous squarylium and cyanine-TCNQ films were so smooth that surface reflectances were as high as 0.7, especially in the 750–850-nm region. The use of antireflective coatings could eliminate the loss of most of this potentially absorbable energy. Also recall that the recoverable wavelengths (750–850 nm) are those where the quantum efficiency for charge generation is maximum or nearly so, as may be seen from the response spectrum in Fig. 6. Thus, the use of an antireflective coating is expected to enhance conversion efficiencies by yielding larger photocurrents.

There are surface morphologies, e.g., [49], which can cause incident light to be reflected and reabsorbed within the films, leading to multiple absorption passes. This allows for a more efficient use of, for instance, thin films that would otherwise absorb only part of the light, but which would be more efficient at transporting and collecting photo-generated carriers. It has been possible to deposit amorphous films of OHSq on dendritic tungsten surfaces, and, indeed, the absorption properties of the resulting films are enhanced if the films remain amorphous.

Another method for effecting at least two light passes would be to use a mirror or other totally reflecting material on the back surface (in a backwall cell, under the ohmic collecting electrode). Calculations of efficiency increases of two to five times have been made by Jain [50] for traditional inorganic devices; it is expected that similar increases could be obtained for organic materials as well.

Summary

Schottky barrier cells made of strongly absorbing thin films of amorphous OHSq have shown backwall power conversion efficiencies as high as 0.15% when low intensity, AM0-simulated sunlight was used. Even at sunlight intensities as high as 90-135 mW/cm² (normal bright sunlight at the earth's surface is approximately 100 mW/cm²) the efficiencies were 0.02%; when compared with other organic materials studied in the past, this indicates a considerable improvement in photovoltaic performance. The highest quantum efficiency, measured for a Ga/OHSq/In-O system, was 0.023 at 850 nm; however, quantum efficiencies averaged about 0.015 over the entire visible absorption range (400-850 nm). The backwall conversion efficiencies at 850 nm were typically 0.2%.

Although the related dyes MeSq and diethyl OHSq also showed photovoltaic behavior, these cells gave much poorer conversion efficiencies, possibly because of their increased crystallinity (or crystallite size), or because of improper choice of electrode systems.

Similar photovoltaic cells made from amorphous thin films of cyanine-TCNQ salts gave conversion efficiencies as high as 0.02%, even though these films were much less absorbant than the OHSq films.

These particular organic materials were chosen for study for their absorption and electronic conduction properties, as well as for their ability to be thin-film-cast in an amorphous or glassy state, properties which have been proposed as essential criteria for potentially efficient photovoltaic materials.

The efficiency of these devices was very sensitive to the nature of the normally "ohmic" collecting electrode, and the collection efficiency could be improved by the proper match of metal and organic semiconductor work functions (surface state limitations are recognized). Hybrid electrode systems or thin films of organic conductors may allow one to retain both good electrode conduction and transmission properties at the same time.

In addition, there are several well established techniques that can be used to further enhance the efficiencies. Doping with bromine vapor or DEASP gave fivefold increases in the measured efficiencies of OHSq cells (e.g., 0.05-0.23% for Br), and such increases can result from changes in conductivity, absorption, energy levels, trapping, or series resistance. Frontwall configurations are expected to enhance efficiencies, as are grid electrodes, antireflective coatings, and special surface

morphologies or mirrors which will create internal reflection and reabsorption.

When all of the above points are considered, it seems likely that there are a number of organic photoconductive materials (e.g., photoconductive dyes, highly absorptive conductive polymers) that, when used in the photovoltaic mode, can yield power conversion efficiencies of one percent or more.

Acknowledgments

The author gratefully acknowledges D. B. Sclove, M. D. Shattuck, and R. Champ for providing the squarylium dyes, and H. J. Hovel, F. B. Kaufman, B. A. Scott, and J. M. Woodall for helpful discussions of photovoltaic principles. Special thanks go to H. J. Hovel for AM0 and spectral response measurements of photovoltaic cells.

References and notes

- 1. H. J. Hovel, Solar Energy 19, 605 (1977).
- J. M. Woodall and H. J. Hovel, Appl. Phys. Lett. 30, 492 (1977).
- 3. H. J. Hovel, IBM J. Res. Develop. 22, 112 (1978).
- (a) D. M. Perkins, Adv. Energy Conversion 7, 265 (1968); (b)
 S. Wagner, J. L. Shay, P. Migliorato, and H. M. Kasper, Appl. Phys. Lett. 25, 434 (1974); S. Wagner, J. L. Shay, K. T. Bachmann, and E. Buehler, Appl. Phys. Lett. 26, 229 (1975); (c) A. Fahrenbruch, V. Vasilchenko, F. Buch, K. Mitchell, and R. H. Bube, Appl. Phys. Lett. 25, 605 (1974); (d) see also J. M. Woodall and H. J. Hovel, Research Report RC 5471, IBM Thomas J. Watson Research Center, Yorktown Heights, NY, 1975.
- P. H. Fang, Proceedings of the International Congress on the Sun in the Service of Mankind (Paris, July 1973), p. 111;
 A. I. Rosenblatt, Electronics 47, 99 (1974).
- C. Lanza and H. J. Hovel, IEEE Trans. Electron Devices ED-24, 392 (1977); (b) P. Vohl, D. M. Perkins, S. G. Ellis, R. R. Addiss, W. Hui, and G. Noel, IEEE Trans. Electron Devices ED-14, 26 (1967); (c) S. J. Bass, J. Cryst. Growth 31, 172 (1975); (d) A. E. Blakeslee and S. M. Vernon, IBM J. Res. Develop. 22, 346 (1978, this issue).
- (a) T. L. Chu, S. Chu, K. U. Duh, H. Z. Mollenkopf, and H. I. Yoo, Conference Record, 12th IEEE Photovoltaic Specialists Conference, Baton Rouge, LA, Nov. 1976; (b) G. H. Schwuttke, T. F. Ciszek, K. H. Yang, and A. Kran, IBM J. Res. Develop. 22, 335 (1978, this issue).
- (a) A. K. Ghosh and T. Feng, J. Appl. Phys. 44, 2781 (1973);
 (b) F. Gutmann and L. E. Lyons, Organic Semiconductors, John Wiley & Sons, Inc., New York, 1967, Ch. 1, and Sections 2.10, 2.12-2.14, 2.20, 3.7, 6.10, 6.11, 8.12, 8.13, 10.2, and 10.4, and references therein.
- C. W. Tang and A. C. Albrecht, (a) Mol. Cryst. Liq. Cryst.
 53 (1974); (b) J. Chem. Phys, 62, 2139 (1975); (c) J. Chem. Phys. 63, 953 (1975); and (d) Nature 254, 507 (1975).
- A. K. Ghosh, D. L. Morel, T. Feng, R. S. Shaw, and C. A. Rowe, J. Appl. Phys. 45, 230 (1974).
- M. I. Fedorov and V. A. Benderskii, Fiz. Tekh. Poluprov. 4, 2007 (1970); Sov. Phys.-Semicond. 4, 1720 (1971).
- 12. V. Y. Merritt and H. J. Hovel, Appl. Phys. Lett. 29, 414 (1976)
- 13. After completion of this paper, a paper submitted for publication by workers at Exxon (D. L. Morel, A. K. Ghosh, T. Feng, E. L. Stogryn, P. E. Purwin, R. F. Shaw, and C. Fishman), came to my attention [now published: Appl. Phys. Lett. 32, 495 (1978)]. In this paper, the authors report that conversion efficiencies as high as 0.7% (uncorrected for electrode absorption) have been measured for devices based on merocyanine dyes.

- 14. H. J. Hovel, IBM Thomas J. Watson Research Center, Yorktown Heights, NY, private communication.
- (a) R. H. Bube, Photoconductivity of Solids, John Wiley & Sons, Inc., New York, 1960; Phys. Rev. 83, 393 (1961); (b) H. J. Hovel, Solar Cells, Vol. 11 of Semiconductors and Semimetals, A. C. Beer and R. K. Willardson, eds., Academic Press, Inc., New York, 1975; (c) J. P. McKelvey, Solid State and Semiconductor Physics, F. Seitz, ed., Harper and Row, New York, 1966; (d) S. M. Sze, in Physics of Semiconductor Devices, Wiley-Interscience Publishers, New York, 1960, ch. 8; (e) C. Kittel, Introduction to Solid State Physics, 4th edition, John Wiley & Sons, Inc., New York, 1971, ch. 9, p. 293 and ch. 11, p. 359; (f) G. A. Somorjai, Principles of Surface Chemistry, in Fundamental Topics in Physical Chemistry Series, Prentice-Hall, Inc., New York, 1972.
- 16. M. Kotani and M. Akamatu, Faraday Soc. Discuss. 51, 94 (1971).
- Y. Harada and H. Inokuchi, Bull. Chem. Soc. Japan 39, 1443 (1966).
- A. Terenin and I. Akimov, Z. Phys. Chem. (Leipzig) 217, 307 (1961).
- M. Kochi, Y. Harada, and H. Inokuchi, Bull. Chem. Soc. Japan 40, 531 (1967).
- H. J. Wintle, Conference Record of 1976 IEEE International Symposium on Electrical Insulators (Montreal), p. 248; and Reference 11.
- 21. Measured by W. Grobeman of the IBM Thomas J. Watson Research Center, Yorktown Heights, NY.
- 22. See, for example, the measuring cell used by W. Mehl and N. E. Wolff, J. Phys. Chem. Solids 25, 1221 (1964).
- L. R. Melby, J. R. Harder, W. R. Hertler, W. Mahler, R. E. Benson, and W. E. Mochel, *J. Amer. Chem. Soc.* 84, 3374 (1962).
- 24. The squarylium dyes that were used in these experiments were kindly provided by D. B. Sclove, M. D. Shattuck, and R. Champ of the IBM Research Laboratory, San Jose, CA.
- 25. For references to the preparation and properties of squaric acid and its derivatives, see (a) S. Cohen, J. R. Lacher, and J. D. Park, J. Amer. Chem. Soc. 81, 3480 (1959) and 84, 2919 (1962); (b) R. West, H. Y. Nui, and M. Ito, J. Amer. Chem. Soc. 85, 2584 (1963); (c) Chemistry of the Carbonyl Group, J. Zabicky, ed., Wiley-Interscience Publishers, New York, Vol. 2, p. 241; (d) A. Treibs and K. Jacob, Angew. Chem. 77, 680 (1965); (e) G. Maahs, Ann. Chem. 686, 55 (1965), Angew. Chem. 78, 927 (1966), and Angew. Chem. International Edition in English 5, 888 (1966); (f) H. E. Sprenger and W. Ziegenbein, Angew. Chem. 78, 937 (1966) and Angew. Chem. Int. Ed. Engl. 5, 894 (1966), and 6, 533 (1967).
- E. K. Putseiko, Elementary Photoprocesses in Molecules,
 B. S. Neporant, ed., Consultants Bureau, NY, 1968, p. 281.
- J. H. Lupinski, K. R. Walter, and L. H. Vogt, Jr., J. Mol. Cryst. 3, 241 (1967).
- B. H. Klanderman and D. C. Hoesterey, J. Chem. Phys. 51, 377 (1969).
- A. Rembaum, A. M. Hermann, F. E. Stewart, and F. Gutmann, J. Phys. Chem. 73, 513 (1969).
- These spectra were run by C. Aliotta and E. I. Alessandrini
 of the IBM Thomas J. Watson Research Center, Yorktown
 Heights, NY.
- 31. See, for example, K.-H. Hellwege and A. M. Hellwege, *Epitaxy Data of Inorganic and Organic Crystals*, Landolt-Bornstein, ed., Vol. 8, Springer-Verlag, New York, 1972.

- 32. These solvent systems had been previously studied and used for chlorodiane blue and squarylium dyes by others within IBM; e.g., by R. Larrabee, H. E. Hunziker, San Jose Research Laboratory; M. D. Shattuck, R. Champ, Office Products Division, San Jose, CA; W. J. Heil, D. B. Sclove, Office Products Division, Lexington, KY.
- 33. F. Kaufman and V. Y. Merritt, IBM Thomas J. Watson Research Center, Yorktown Heights, NY, unpublished results.
- 34. P. J. Melz, R. B. Champ, L. S. Chang, C. Chiou, G. S. Keller, L. C. Liclican, R. R. Neiman, M. D. Shattuck, and W. J. Weiche, *Photog. Sci. Eng.* 21, 73 (1977).
- I. Lundstrom, G. A. Corker, and V. Y. Merritt, IBM Thomas J. Watson Research Center, Yorktown Heights, NY, unpublished results.
- P. Melz, IBM San Jose Research Laboratory, CA, unpublished results.
- 37. W. Mehl and N. E. Wolff, J. Phys. Chem. Solids 25, 1221 (1964).
- 38. A. F. Garito and A. J. Heeger, *Accts. Chem. Res.* 7, 232 (1974).
- L. B. Coleman, M. J. Cohen, D. J. Sandman, F. G. Yamagishi, A. F. Garito, and A. J. Heeger, *Solid State Commun.* 12, 1125 (1973).
- 40. E. M. Engler, R. A. Craven, Y. Tomkiewicz and B. A. Scott, J. Chem. Soc. Chem. Commun., 337 (1976).
- 41. H. Shirakawa, E. J. Louis, A. G. MacDiarmid, C. K. Chiang, and A. J. Heeger, *J. Chem. Soc. Chem. Commun.* 578 (1977), and unpublished results.
- P. J. Reucroft, K. Takahashi, and H. Ullal, Appl. Phys. Letters 25, 664 (1974); J. Appl. Phys. 46, 5218 (1975).
 J. H. Lupinski and K. D. Kopple, Science 146, 1038 (1964);
- J. H. Lupinski and K. D. Kopple, Science 146, 1038 (1964);
 J. H. Lupinski, K. D. Kopple, and J. J. Hertz, J. Polymer Sci., 1561 (1967).
- 44. A. Rembaum, W. Baumgartner, and A. Eisenberg, *Polymer Lett.* 6, 159 (1968).
- 45. Work function values of elements are taken from: H. B. Michaelson, J. Appl Phys. 48, 4729 (1977).
- See, for example, A. E. Ennos, Brit. J. Appl. Phys. 8, 113 (1957), and unpublished results of E. M. Da Silva and F. Kaufman of the IBM Thomas J. Watson Research Center, Yorktown Heights, NY.
- 47. H. J. Hovel and V. Y. Merritt, IBM Thomas J. Watson Research Center, Yorktown Heights, NY, unpublished work.
- (a) D. Amingual, C. Motie, T. Nguyen-Duy, S. Mottet, A. Roizes, R. Schuttler, and W. Palz, Proceedings of the International Congress on the Sun in the Service of Mankind, Paris, July 1973, p. 61; (b) M. A. Green, App. Phys. Lett. 27, 287 (1975).
- 49. G. D. Pettit, J. J. Cuomo, T. H. DiStefano, and J. M. Woodall, *IBM J. Res. Develop.* 22, 372 (1978, this issue).
- V. K. Jain and S. C. Jain, *Phys. Status Solidi A* 30, K69 (1975);
 S. C. Jain, *Proc. Roy. Soc.* 243, 359 (1958).

Received February 8, 1978; revised March 23, 1978

The author is located at the IBM Corporate Headquarters, Armonk, New York 10504.